

## Theoretical Determination of Forming Limit Stress Diagram for Steel 1021 Sheet

Anas O. Balod

Mechanical Engineering Department, Mosul University

### Abstract

Forming limit stress diagram represent the maximum acceptable limits of principal stresses in sheet metal forming. This diagram show the limits of major and minor true stresses for different strain paths (uniaxial tension, plane strain and equibiaxial stretching path) in sheet metal forming. It is confirmed that the Forming limit stress diagram and the Forming Limit Strain Diagram are two mathematically equivalent representations of forming limits in stress space and strain space respectively. The Forming limit stress diagram of the sheet metal is gained by the transformation relations between the strain state and stress state in deformation of sheet metal. In this paper, the Forming limit stress diagram is theoretically determined using Marciniak-Kuczynski analysis and Hosford yield criterion for steel 1021 sheet ,and compared with the experimental Forming limit stress diagram based on the experimental Forming limit strain diagram of steel 1021 sheet & theory of plasticity. The influence of normal anisotropic ratio, index of yield criterion, inhomogeneous factor and strength coefficient on the theoretical FLSD is also presented. It is shown that the limit stresses in theoretical Forming limit stress diagram is raised by increased values of the normal anisotropic ratio, the inhomogeneous factor and the strength coefficient. The limit stresses are lowered when the index of Hosford yield criterion increased.

**Keyword:** Forming limit stress diagram , M-K analysis, Hosford yield criterion

التعيين النظري لمخطط حد إجهاد التشكيل لصفحة من الصلب (1021)

الخلاصة:

يمثل مخطط حد إجهاد التشكيل الحدود العظمى المقبولة للاجهادات في تشكيل الصفائح المعدنية. يبين هذا المخطط حدود الإجهاد الحقيقي الرئيسي والثانوي عند مسارات مختلفة (مسار الشد أحادي المحور، مسار الانفعال المستوي وكذلك مسار الشد ثنائي المحور المتساوي) عند تشكيل الصفائح المعدنية. من المعروف إن مخطط حد إجهاد التشكيل ومخطط حد التشكيل يمثلان التعبير الرياضي المكافئ لحدود التشكيل (حدود الإجهادات، حدود الانفعالات). يمكن الحصول على مخطط حد إجهاد التشكيل للصفائح المعدنية من استخدام العلاقات التحويلية بين الإجهاد والانفعال (نظريات اللدونة). في هذا البحث تم تعيين مخطط حد إجهاد التشكيل نظريا باستخدام تحليل (Marciniak-Kuczynski) ونظرية الخضوع (Hosford) لصفحة من الصلب 1021، ومقارنته مع مخطط العملي لحد إجهاد التشكيل (تم تعيينه بواسطة مخطط حد الانفعال العملي لصفحة الصلب 1021 ونظريات اللدونة). وكذلك تمت دراسة تأثير كل من معامل تباين الخواص وقيمة أس نظرية الخضوع (Hosford) ومعامل عدم التجانس ومعامل مقاومة المعدن على المخطط النظري لحد إجهاد التشكيل. حيث أظهرت النتائج إن حدود الإجهاد ترتفع عند زيادة كل من معامل تباين الخواص ومعامل عدم التجانس ومعامل مقاومة المعدن، بينما تنخفض حدود الإجهاد عند زيادة قيمة أس معادلة الخضوع.

**Notation**

<b>Symbol</b>	<b>Definition</b>
$\sigma_1, \sigma_2, \sigma_3$	Principal stresses, MPa
$\epsilon_1 \epsilon_2 \epsilon_3$	Principal strains
$m$	Strain rate sensitivity
$n$	Strain hardening exponent
$\sigma'$	effective stress, MPa
$\dot{\epsilon}$	effective strain
$\dot{\epsilon}$	strain rate
	1/sec
$\dot{\epsilon}$	effective strain rate, 1/sec
$\rho$	ratio of minor strain to major strain
$t_a$	thickness of the sheet
$t_b$	Thickness of groove
$\alpha$	Principle stress ratio
$f$	Imperfection factor
$a$	Yield criterion index
$K$	Strength coefficient, MPa
$R'$	Normal plastic anisotropic, ratio
$R_0$	Plastic anisotropic ratio with rolling direction
$R_{90}$	Plastic anisotropic ratio transverse to rolling direction
$\phi$	ratio of principal stress to effective stress
$\beta$	Ratio of effective strain to principal strain
M-K	Marciniak-Kuczynski analysis
$F_{1a}$	Principal Force in region (a) in M.K Analysis, N
$F_{1b}$	Principal Force in region (b) in M.K Analysis, N

**Introduction**

The sheet metal formability is a measure of its ability to be deformed plastically during a forming process in order to produce a part with definite shape, being mainly limited by the occurrence of flow localization or instability. Its strong dependence on both the intrinsic constitutive properties of the sheet metal and the extrinsic factors involved in a practical forming operation made the correct choice of these parameters to be one of the main aims in modern industry. Their experimental study is difficult and sometimes infeasible task. The theoretical analysis of plastic instability is therefore of major importance to predict the appearance of localized necking, to examine the influence of each parameter on the necking occurrence and to improve the press performance. A good understanding of the deformation processes, of the plastic flow localization and of the factors limiting the forming of

sheet metal is crucial in monitoring the formability issue<sup>[1]</sup>.

Arrieux et al.(1982) are the first who studied the forming limit stress states concerns the isotropic materials using Von Mises yield criterion.

Gronostajski et al.(1984) studied the forming limit stress diagrams in axes of anisotropic sheets using Hill's non quadratic criteria for aluminum and ARMCO iron sheet.

Arrieux et al.(1990) plotted the theoretical forming limit stress curve determined by means of the two zoned Marciniak's model which is developed in order to give the stress states in the two areas. It was concluded that all FLSDs, based on phenomenological plasticity models such as Hill (1948) and Hosford(1979), were almost path-independent (Arrieux, (1995), Zhao et al., (1996), Haddad et al.,(2000), Stoughton, (2000), Zimniak, (2000), Stoughton and Zhu, (2004) In a preliminary study on the

FLSD based on crystal plasticity, Wu et al. (2000) came to a similar conclusion. stresses based on a polycrystalline plasticity theory, assuming isotropic hardening on each slip system, in conjunction with the Marciniak and Kuczynski model (M-K model; Marciniak and Kuczynski, 1967).

Butuc et al. (2006) study the effect of work hardening coefficient, strain rate sensitivity and the balanced biaxial yield stress on the theoretical FLSD by using M-K analysis and different yield function (groove orientation method). Yoshida et al. (2005) measured the forming limit strains and stresses of an A5154-H112 tube for many linear and combined stress paths, using a servo-controlled, internal pressure-axial load testing machine. Yoshida et al. (2007) also calculated the forming limit stresses for many two-stage combined stress paths by using the M-K model and a phenomenological plasticity theory with the isotropic hardening rule. Yoshida et al. (2007) explained that the path-independence of the FLSC is attributed to the isotropic hardening rule used in the constitutive model.

This work discusses the comparison between theoretical and experimental FLSD (based FLD & theory of plasticity) for Steel 1021 sheet, and the influences of normal anisotropic ratio, index of yield criterion, inhomogeneous factor and strength coefficient on the theoretical FLSD were studied

**Mechanical property of Steel 1021 sheet:**

The mechanical properties of steel 1021 sheet were obtained from tensile test, by using specimens at different angles (0°, 45°, 90°) to the rolling direction Table(1). The value of strain hardening

In numerical studies, Wu et al. (2000, 2005) calculated the forming limit exponent (n) was determined from the slope of line in the (log coordinate of true stress-strain curve) by selection two points, one before ultimate stress and the other after yield point. The intersection of this line with unit strain gives the stress value that define the magnitude of strength coefficient (K)<sup>[1]</sup>. To determine the anisotropy plastic ratio (R) the same specimens of tensile test were used with different angles and using equation (1) (table 1) and the equation (2) to determine the normal anisotropic ratio<sup>[1]</sup>.

$$R = \frac{\epsilon_w}{\epsilon_t} \dots\dots\dots(1)$$

Where  $\epsilon_w$ : strain in the width direction of the specimen,  $\epsilon_t$ : strain in the thickness direction of the specimen.

$$R' = \frac{R_0 + 2R_{45} + R_{90}}{4} \dots\dots\dots(2)$$

The strain rate sensitivity (m) was determined by using the same tensile test specimens. The cross-head speed is suddenly changed during the uniform deformation region of a tensile test and a small jump in the load may be observed. The exponent (m) is then calculated (eq.3) from load and cross-head speed before and after the speed change<sup>[1]</sup>.

$$m = \frac{\log\left(\frac{P_1}{P_2}\right)}{\log\left(\frac{V_1}{V_2}\right)} \dots\dots\dots(3)$$

Where  $P_1$ : load before the speed change.,  $P_2$ : load after the speed change.

$V_1$ : cross head speed before the speed change,  $V_2$ : cross head speed after the speed change.

The values of n, m, R and K, were found experimentally which are shown in table (1).

To determine the mean of mechanical property of the steel 1021 sheet using equation(4).

$$X = \frac{X_0 + 2X_{45} + X_{90}}{4} \dots\dots\dots(4)$$

Table (2) present the mean of mechanical property (n, m, K and R'), which were used in the determination of FLSD.

**Theoretical Analysis:**

The theoretical forming limit stress diagrams presented in this work were calculated using a more general code(M-K analysis and Theory of plasticity) for predicting the forming limits under linear strain paths. The code consists of a main part and several subroutines allowing the implementation of hardening law, yield function. Its general structure of theoretical FLSD is shown in Fig. 1.

The geometry of neck formation and the element of sheet undergoing plastic deformation are shown in Fig.2. Following the MK analysis, based on a simplified model with assumed pre-existing thickness imperfection in the form of a groove perpendicular to the principal stress directions, The sheet is composed of the nominal area and weak groove area, which are denoted by 'a' and 'b', respectively. The initial imperfection factor of the groove,  $f_0$ , is defined as the thickness ratio ( $f_0 = t_{ob}/t_{oa}$ ); where (t) denotes the thickness and subscript (o) denotes the initial state. A biaxial stress state is imposed on the nominal area and causes the development of strain increments in both the nominal (a) and the weak area (b).

The yield criterion proposed by Osford<sup>[6]</sup> was used in the calculation in the plane stress state, this criterion is obtained as follows:

$$(\sigma')^a = \frac{1}{(R'+1)} [(\sigma_1)^a + (\sigma_2)^a + R'(\sigma_1 - \sigma_2)^a] \dots\dots\dots(5)$$

using a = 6

The behavior of material can be represented in the form of Power law

$$\sigma' = K \varepsilon'^n \dot{\varepsilon}'^m \dots\dots\dots(6)$$

The ratio of the principal stress and strain is defined as follows:

$$\alpha = \frac{\sigma_2}{\sigma_1}, \rho = \frac{\varepsilon_2}{\varepsilon_1} = \frac{d\varepsilon_2}{d\varepsilon_1} \dots\dots\dots(7)$$

The associated flow rule is expressed by

$$d\varepsilon_{ij} = d\lambda \frac{\partial \sigma'}{\partial \sigma_{ij}} \dots\dots\dots(8)$$

$$\text{and } d\varepsilon_1 = \frac{d\varepsilon' \varphi^{a-1}}{(R+1)} [1 + R(1-\alpha)^{a-1}] \dots\dots(9)$$

$$d\varepsilon_2 = \frac{d\varepsilon' \varphi^{a-1}}{(R+1)} [(\alpha)^{a-1} - R(1-\alpha)^{a-1}] \dots\dots(10)$$

Using condition of constant volume in plastic deformation

$$d\varepsilon_1 + d\varepsilon_2 + d\varepsilon_3 = 0 \dots\dots\dots(11)$$

from eq.(11)

$$d\varepsilon_3 = -\frac{d\varepsilon' \varphi^{a-1}}{(R+1)} [1 + (\alpha)^{a-1}] \dots\dots\dots(12)$$

then, by applying the principle of equivalence of plastic work

$$\sigma'd\varepsilon' = \sigma_1 d\varepsilon_1 + \sigma_2 d\varepsilon_2 \dots\dots\dots(13)$$

the compatibility condition is given by

$$d\varepsilon_{2a} = d\varepsilon_{2b} \dots\dots\dots(14)$$

from Marciniak-Kuczynski analysis [15].

$$f = \frac{t_b}{t_a} \dots\dots\dots(15)$$

$$f = f_o \exp(\varepsilon_{3b} - \varepsilon_{3a}) \dots\dots\dots(16)$$

the equilibrium condition requires that the applied load remains constant along the specimen ; therefore

$$F_{1a} = F_{1b} \dots\dots\dots(17)$$

from eq.(6),(17)

$$\varphi_a (\varepsilon'_a + d\varepsilon'_a)^n \dot{\varepsilon}'_a{}^m = f\varphi_b (\varepsilon'_b + d\varepsilon'_b)^n \dot{\varepsilon}'_b{}^m \dots(18)$$

Equilibrium equation (14), an equation can be found and solved numerically. Imposing a loading path (pa), a finite increment of strain is also imposed in region (a), and by numerical computation is performed by using computer program (Fortran power Station) to determine the limit stress of a strain path in the FLSD , and the limit strain is determined when [(deb1/dεa1) > 10] in the range of strain ratios from (-0.7 to 1.0).

**Calculation of Stress-based forming Limits Based on Experimental Strain Data**

The stress-based forming limit curve represents the forming limit diagram expressed using the principal stress components in-plane of the sheet. The stress states cannot be determined directly on experimental parts and this operation generally needs a plastic calculation. Based on the experimental forming limit strains and using the plasticity theory, the forming limit stresses are computed[16]. It is assumed that the principal anisotropy axes of orthotropic symmetry are coincident with the principal axes of stress. In this paper we can use major true

strain and strain ratio(Eq.19) from forming limit strain diagram for the same material,

$$\rho = \frac{\varepsilon_2}{\varepsilon_1} \dots\dots\dots(19)$$

and with using plasticity theory that presented by Hosford yield function (Eq.19)[6] , plastic work (Eq.20) and hardening law (power law) (Eq.22).

$$(\sigma')^a = \frac{1}{(R' + 1)} [(\sigma_1)^a + (\sigma_2)^a + R'(\sigma_1 - \sigma_2)^a] \dots\dots\dots(20)$$

$$\sigma'd\varepsilon' = \sigma_1 d\varepsilon_1 + \sigma_2 d\varepsilon_2 \dots\dots\dots(21)$$

and with hardening law (power law)

$$\sigma' = K\varepsilon'^n \dots\dots\dots(22)$$

and the stress ratio:

$$\alpha = \frac{\sigma_2}{\sigma_1} \dots\dots\dots(23)$$

For cases with non shear stress in a coordinate system aligned with the axes of anisotropy, the major true stress can be expressed as follows:

$$\sigma_1 = \sigma'(\varepsilon') \times \varphi(\alpha) \dots\dots\dots(24)$$

where  $\sigma'(\varepsilon')$  represents the effective stress computed through the hardening law, and  $\varphi(\alpha)$  is a function of material parameters derived from the applied yield criteria. the effective strain is obtained for Hosford yield criteria[6] through the corresponding plastic strain in this paper, and calculating the minor true stress using the stress ratio(Eq.(23)).

The above equations show that the experimental forming limit stress diagram depends on the shape of the yield surface as well as the hardening law used to describe the work hardening material behavior.

### Results and Discussion :

Figure(3) show the forming limit strain diagram of steel 1021 sheet determined experimentally by stretch forming using hemispherical punch, the limit strain in uniaxial tension path is higher than the limit strain in equibiaxial tension path while the limit strain lowest in plane strain path. Figure (4) show the experimental forming limit stress diagram of steel 1021 sheet obtained on the basis of the experimental forming limit strain diagram (figure.3) and plastic theory (using Hosford yield function ( $a=6$ )), the limit stress in equibiaxial tension path is higher than limit stress in uniaxial tension path while the limit stress lowest in plane strain path.

Figure(5) show the comparison between the experiment and theoretical forming limit stress diagram using Hosford yield function (high exponent.  $a=6$ ) with M-K analysis. It can be seen that the theoretical FLS curve more approach to the experimental FLS curve in plane strain path and approach in both paths of equibiaxial tension and uniaxial tension path.

Figure(6) show the influence of the normal anisotropy ratio ( $R'$ ) on the limit stress of FLSDs, presenting several curves predicted by use different values of normal anisotropy ratio (0.5, 0.8, 1.44 and 2). It is observed that the level of the FLSD depends on the normal anisotropy ratio. When the normal plastic anisotropy increases the predicted of forming limit stress curve is increased, but the effect of normal plastic anisotropy ratio in forming limit strain diagram is independent by using Hosford yield function ( $a=6$ )<sup>[19]</sup>. The difference between curves in uniaxial tension path are more than in

equibiaxial tension path, and can be seen that the effect of normal plastic anisotropy ratio in uniaxial tension path is more than in equibiaxial tension path. While this increase in normal plastic anisotropy ratio ( $R'$ ) mean that the width strain is greater than thickness strain and associated with a greater resistance to forming in the thickness direction (resistance to thinning).

Figure (7) shows the influence of index of Hosford yield function on forming limit stress diagram. It is observed that the level of the FLSD strongly depends on the selection of index of hosford yield function by using different values of index (2, 6 and 8). When the index of hosford yield criterion increases, the predicted forming limit stress decrease. More stable of curves at increase the index of hosford yield function, and the index (2) is difference than curves because the index (2) reference to Hill yield criterion.

Figure (8) shows the effect of initial value of inhomogeneous factor in M.K analysis on the limit stress in the forming limit stress diagram. It is observed that the limit stress of the FLSD strong sensibility depends on the selection of initial value of inhomogeneous factor, several curves predicted by use different values of initial value of inhomogeneous factor (0.98, 0.99 and 0.998). The level of the predicted forming limit stresses rises when the initial inhomogeneous factor increases. Presenting the same behavior like the one achieved by the forming limit strains concerning the respective dependence as was shown in previous studies<sup>[19],[20]</sup>. It is important to remark, once again, that even the initial geometrical factor is considered an adjustable parameter in order to achieve

the best accuracy in the predicted forming limit stress diagram. The initial inhomogeneous value in M-K analysis represent the ratio of initial imperfection thickness to initial normal thickness ( $f_0 = t_{ob}/t_{oa}$ ), and when the initial inhomogeneous value ( $f_0$ ) increase the imperfection thickness ( $t_{ob}$ ) in (M-K) analysis is increase and cause increase in the limit stress in FLSD for all paths.

Figure (9) show the effect of Strength coefficient (K) on forming limit stress diagram, it is observed that the level of the FLSD depends on the selection of Strength coefficient. presenting several curves predicted by use different values of Strength coefficient (400,600 and 800MPa).When the Strength coefficient increases the predicted forming limit stress curve is increased for all paths with different level. The effect of strength coefficient presented in hardening law(power law), and hardening law play a vital role and very important to calculate the limit stress of forming limit stress diagram.

#### Reference:

1. Marciniak, Z., Duncan, J.L., "Mechanics of Sheet Metal Forming", 2nd edition, Butter worth-Heinemann, (2002).
2. Arrieux R, Bedrin C, Boivin M., "Determination of an Intrinsic Forming Limit Stress Diagram for Isotropic Sheets", In Proceedings of the 12th IDDRG congress, Santa Margherita, Ligure, Vol.2, pp. 61–71, (1982).
3. Gronostajski, I., "Sheet Metal Forming Limits for Complex Strain Paths", J. Mech. Work. Tech., Vol.10 (3), pp. 349–362 (1984).
4. Arrieux et al, "Determination of the Forming Limit Stress Curve for Anisotropic Sheets", Annals of the CIRP, Vol.36, pp.235, (1990).
5. Hill, R., "A Theory of the Yielding and Plastic Flow of Anisotropic Metals", Proceedings of the Royal Society of London Series A-Mathematical, Physical and Engineering Science A193, 281–297, (1984).
6. Hosford, W.A., "On Yield Loci of Anisotropic Cubic Metals", In Proceedings of the 7th North American Metalworking Conference, SME, Dearborn, MI, pp. 191–197, (1979).
7. Arrieux, R., "Determination and Use of the Forming Limit Stress Diagrams in Sheet Metal Forming", Journal of Materials Processing Technology ,Vol.53, pp. 47–56, (1995).
8. Zhao, L.R., Sowerby, R., Sklad, M.P., "A Theoretical and Experimental Investigation of Limit Strains in Sheet Metal Forming", Int. J. Mech. Sci., Vol.38 (12), pp. 1307–1317, (1996).
9. Haddad, A., Arrieux, R., Vacher, P., "Use of Two Behavior Laws for the Determination of the Forming Limit Stress Diagram of a Thin Steel Sheet: Results and Comparisons", Journal of Materials Processing Technology ,Vol. 106, pp. 49–53, (2000).
10. Stoughton, T.B., "A General Forming Limit Criterion for Sheet Metal Forming", Int. J. Mech. Sci., Vol. 42 (1), pp. 1–27, (2000).
11. Zimniak, Z., "Application of a System for Sheet Metal Forming Design", J. Mater. Process, Vol. 106, pp. 159–162, (2000).
12. Stoughton, T.B., Zhu, X., "Review of Theoretical Models of the Strain-based FLD and their Relevance to the Stress-Based FLD", International Journal of Plasticity, Vol. 20, pp. 1463–1486, (2004).

13. Wu, P.D., Graf, A., Jain, M., MacEwen, S.R., "On Alternative Representation of Forming Limits", *Key Engineering Materials*, Vol. 177–180, pp. 517–522, (2000).
14. Wu, P.D., Graf, A., Jain, M., MacEwen, S.R., "On Forming Limit Stress Diagram Analysis", Vol. 42, pp. 2225-2241, (2005).
15. Marciniak Z, Kuckzinsky K., "Limit Strains in the Processes of Stretch Forming Sheet Metal", *International Journal of Mechanical Sciences*, Vol.9, pp. 609–620 (1967).
16. Butuc MC, Barata da Rocha A, Gracio JJ. "An Experimental and Theoretical Analysis on the Application of Stress-based Forming Limit Criterion", *International Journal of Mechanical Sciences*, vol. 48, pp. 414-429, (2006).
17. Yoshida, K., Kuwabara, T., Narihara, K., Takahashi, S., "Experimental Verification of the Path-dependence of Forming Limit Stresses", *Int. J. Forming Processes*, vol.8 (SI),pp. 283–298,(2005).
18. Yoshida, K., Kuwabara, T., "Effect of Strain Hardening Behavior on Forming Limit Stresses of Steel Tube Subjected to non Proportional Loading Paths", *Int. J. Plasticity*, vol. 23 (7), pp. 1260–1284, (2007).
19. Graf, A. and Hosford, W.F., "Calculations of Forming Limit Diagrams", *Metall. Trans.*, vol. 21A, pp. 87-96, (1990).
20. Grootenboer. H. J., Huetink. H. J, "Thermally Enhanced Forming of Aluminium Sheet Modelling and Experiments", A. H. Van den Boogaard ,Hengelo, the Nether Lands, pp. 83-87, (2002).

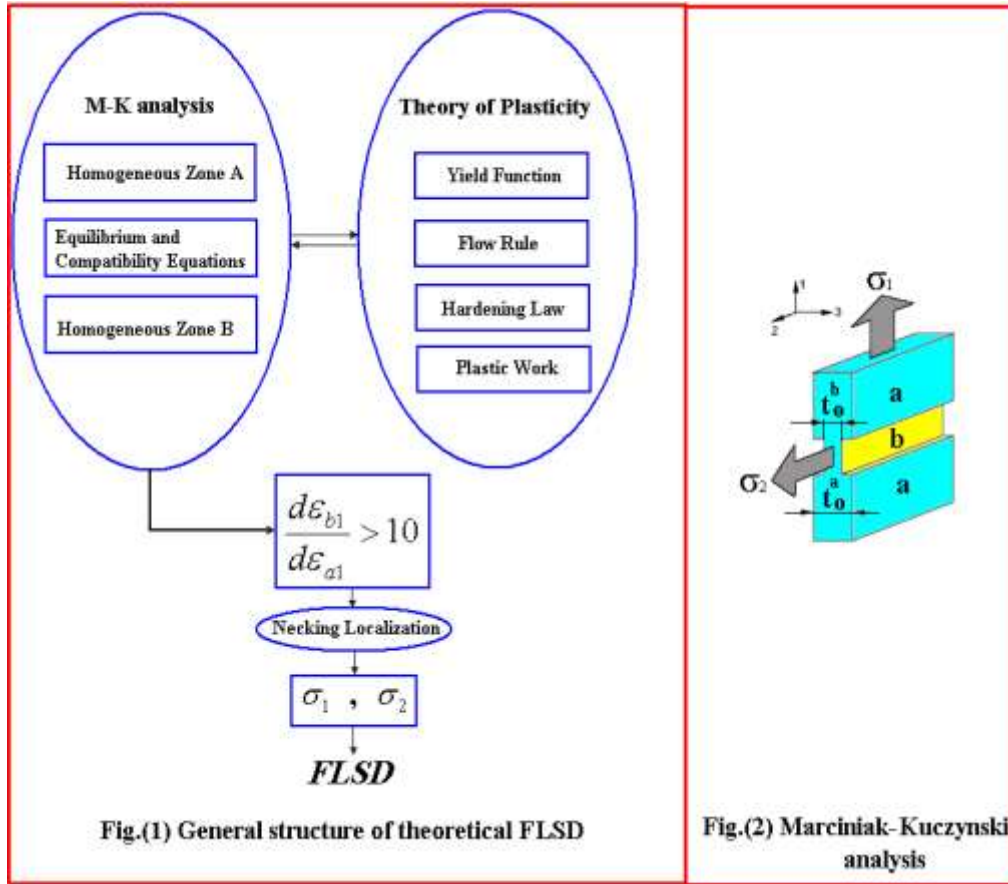


Fig.(1) General structure of theoretical FLSD

Fig.(2) Marciniak-Kuczynski analysis

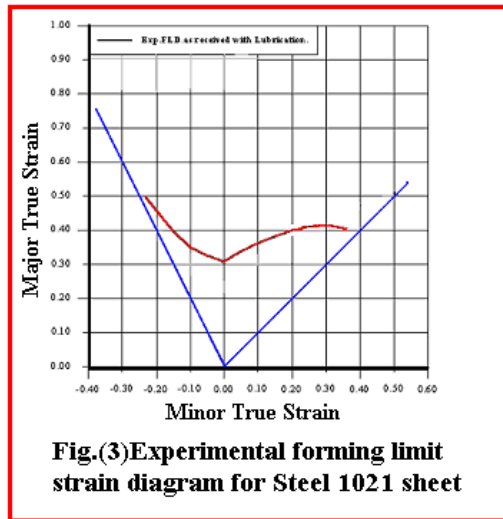


Fig.(3) Experimental forming limit strain diagram for Steel 1021 sheet

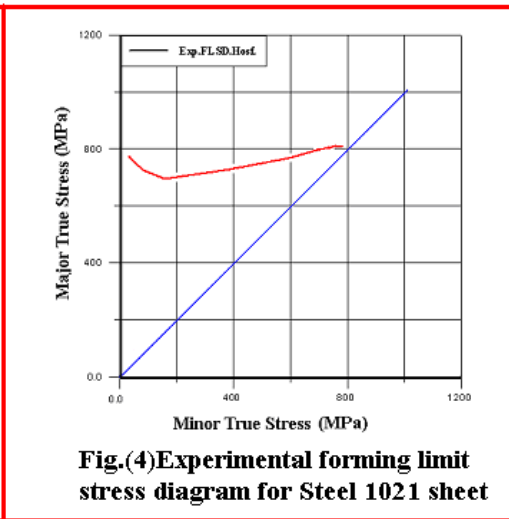


Fig.(4) Experimental forming limit stress diagram for Steel 1021 sheet

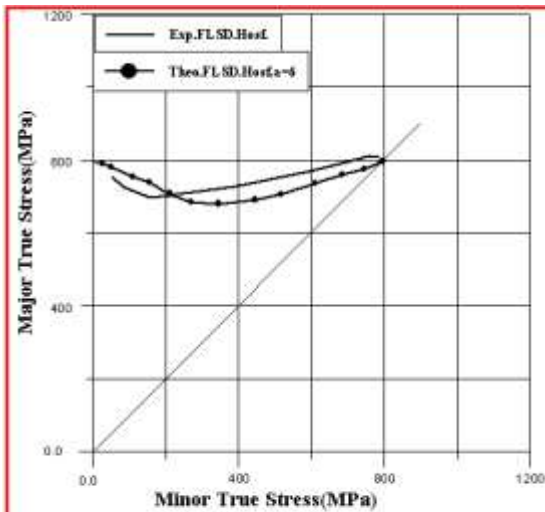


Fig.(5) Comparison between the experimental and theoretical forming limit stress diagram for Steel 1021 sheet

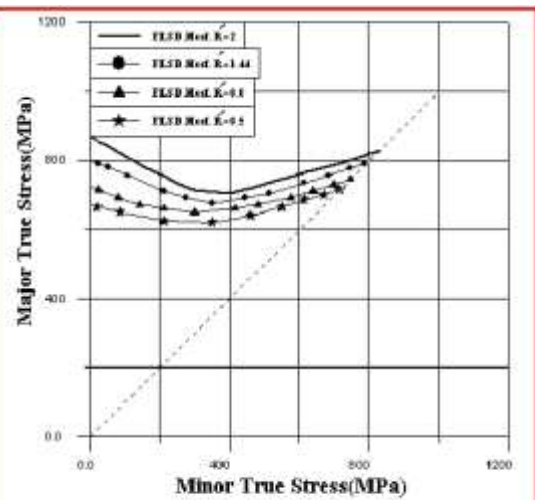


Fig.(6) The effect of the normal plastic anisotropy ratio on theoretical FLSD

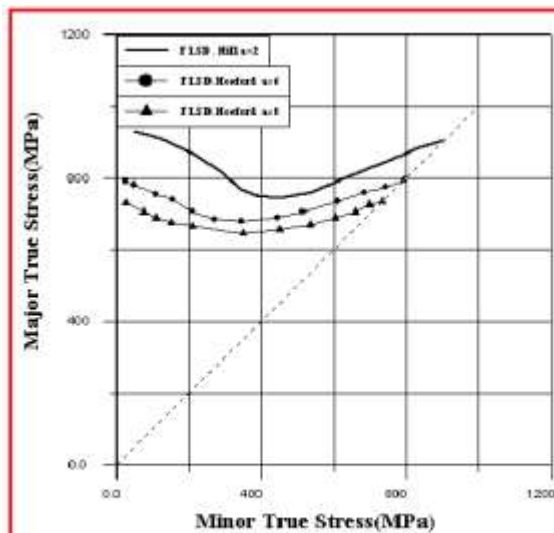


Fig.(7) The effect of the index of Hosford yield criterion on theoretical FLSD

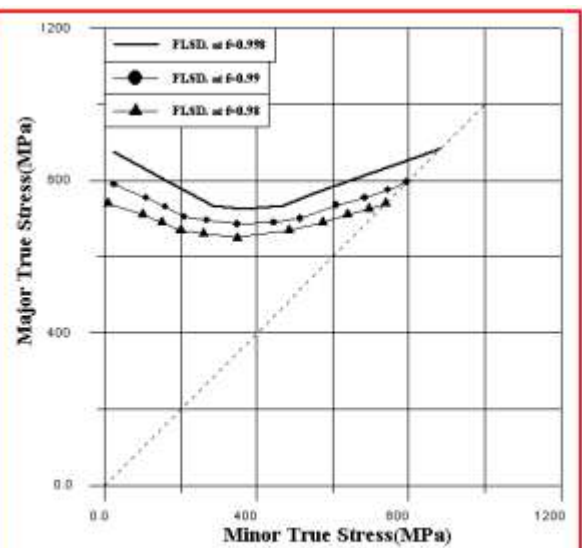
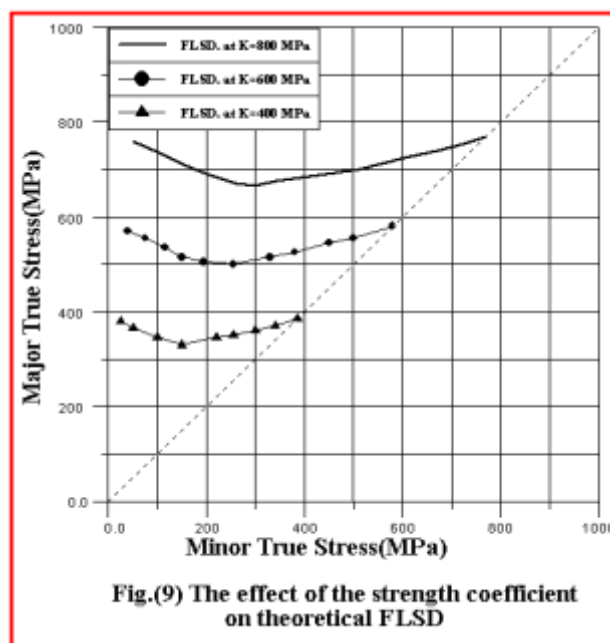


Fig.(8) The effect of the initial inhomogeneous factor on theoretical FLSD



**Table (1) Property of the Steel 1021 sheet**

Material	Angle between specimens axis and rolling direction	Strain Hardening exponent (n)	Strain rate sensivity (m)	plastic Anisotropic ratio (R)	Strength coefficient (K)[MPa]
Steel 1021	0°	0.282	0.018	1.7511	820
	45°	0.254	0.013	1.2521	790
	90°	0.265	0.016	1.5419	810

**Table(2)Mean of mechanical property**

Material	Mean of strain Hardening exponent (n)	Mean of strain rate sensivity (m)	Normal plastic anisotropic ratio (R)	Mean of strength coefficient [MPa]
Steel 1021	0.26375	0.015	1.4493	802.5

